Journal of Applied Polymer Science

Taurine as an additive for improving the fouling resistance of nanofiltration composite membranes

Jinbo Jin, Dongqing Liu, Dandan Zhang, Yuhang Yin, Xinyu Zhao, Yufeng Zhang
State Key Laboratory of Hollow Fiber Membrane Materials and Processes, School of Material Science and Engineering, Tianjin Polytechnic University, Tianjin 300387, China
Correspondence to: D. Liu (E-mail: ldqnov@163.com)

ABSTRACT: A hydrophilic compound, taurine, was investigated as an additive in the interfacial polymerization between piperazine (PIP) and trimesoyl chloride (TMC) to prepare thin-film composite (TFC) membranes. The resulting membranes were characterized by X-ray photoelectron spectroscopy and attenuated total reflectance–Fourier transform infrared spectroscopy. The morphology and hydrophilicity of the membranes were investigated through scanning electronic microscopy and water contact angle measurements. The separation performance of the TFC membranes was investigated through water flux and salt rejection tests. The protein-fouling resistance of the films was evaluated by water recovery rate measurements after the treatment of bovine serum albumin. The membrane containing 0.2 wt % taurine showed the best performance of 92% $MgSO_4$ rejection at a flux of 31 L m^{-2} h^{-1} and better antifouling properties than the PIP–TMC membranes. An appropriately low concentration of taurine showed the same $MgSO_4$ rejection as the PIP–TMC membranes but a better fouling resistance performance. © 2014 Wiley Periodicals, Inc. J. Appl. Polym. Sci. **2015**, *132*, 41620.

KEYWORDS: crosslinking; hydrophilic polymers; membranes; polyamides; separation techniques

Received 4 July 2014; accepted 9 October 2014
DOI: 10.1002/app.41620

INTRODUCTION

The increasing concern over the exhaustion of natural clean water and energy has driven humanity to search for alternative supplies. The desalination of seawater or the treatment of brackish water becomes one promising approach for providing consumable water. Among the tremendous tests, nanofiltration (NF) was confirmed as an effective technique for desalination and could also be used in liquid purification, sewage, and industrial wastewater treatments because of its low pressure requirement.[1–3]

As a membrane separation process, the NF technique is green and effective.[4–6] However, the widespread use of this technique is limited by membrane fouling, particularly biofouling.[7–9] Fouling is usually caused by the adsorption or deposition of microorganisms on the membrane surface or in membrane pores and is then followed by microorganism reproduction and ultimately the formation of a sticky biofilm; this could seriously destroy the permeation properties of the membranes.[10,11]

Currently developed nanofiltration membranes (NFMs) are thin-film composite (TFC) membranes composed of a dense selective layer on the top of a porous support. Active top-layer screening is an important research field. The improvement of the surface hydrophilicity has been confirmed to be effective in the development of antifouling-resistant surfaces. The introduction of hydrophilic compounds onto membrane surfaces is a convenient method for preparing TFC membranes during interfacial polymerization (IP) without a significant loss in the salt rejection (R) capability.[12] Zhao *et al.*[13] incorporated dopamine in the polycondense with trimesoyl chloride (TMC) *n*-hexane as an organic phase on a poly(ether sulfone) ultrafiltration (UF) substrate to prepare composite membranes. The resulting NFM was chemically stable in ethanol and sodium hypochlorite solutions. Li *et al.*[14] reported a novel NF composite membrane prepared through poly(hexamethylene guanidine hydrochloride) (PHGH) and TMC coated on a polysulfone (PSF) UF membrane by IP. The resulting film demonstrated an enhanced antibiofouling performance. Zhao *et al.*[15] confirmed that *o*-aminobenzoic acid–triethylamine salt, a monofunctional hydrophilic compound, improved the antifouling performance of the composite membrane as an ingredient of IP. Kim *et al.*[16] added tributyl phosphate or triphenyl phosphate into a TMC solution to prepare polyamide (PA) TFC membranes. Tributyl phosphate membranes showed better performance than both piperazine (PIP) and triphenyl phosphate membranes. Kuehne *et al.*[17] reported that the addition of camphor sulfonic triethylamine salt increased the water flux (F) of composite membranes and maintained a high R. In a word, the proper content of monofunctional additives is valuable in the improvement of the

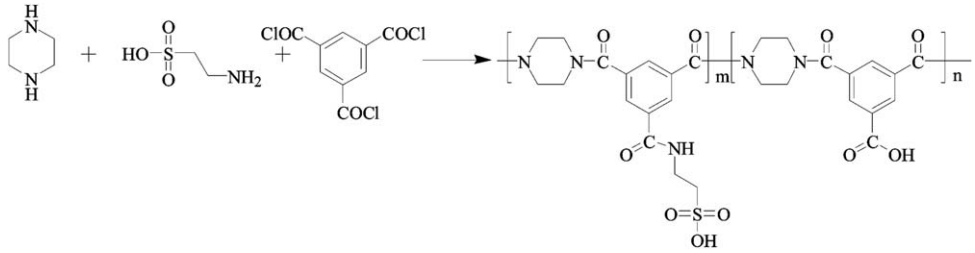

Figure 1. Probable chemical structures of the surface membranes.

surface hydrophilicity and maintenance of *R*. A high surface hydrophilicity is effective in improving the pollution resistance of the membrane.

Hydrophilic monomer for composite membranes should include two factors: (1) reactive groups and (2) hydrophilic groups.[18] Taurine (Figure 1), a water-soluble compound, contains both reactable amino and sulfonic acid group in one structure, which made it a promising additive for composite membrane in IP. In this work, NF composite membranes were fabricated using the blend aqueous solution of taurine and PIP to polycondense with TMC. NF performance and membranes fouling resistance was investigated to evaluate the effect of taurine in the chemistry of film surface.

EXPERIMENTAL

Materials

TMC (>99%), PIP (>99.5%), and *n*-hexane were obtained from Sinopharm Chemical Reagent. Taurine was purchased from J&K Chemical. NaCl and $MgSO_4$ were purchased from Kermel Chemical Reagent Co., Ltd. (Tianjin, China) and used without any further purification. Bovine serum albumin (BSA) was purchased from Shanghai Aladdin Reagent Co. Phosphate-buffered saline was purchased from Sigma. The PSF–UF sheet membrane (molecular weight cutoff = 20,000) with nonwoven fabric support was supplied by GE Co.

Preparation of the Polyamide Membranes

IP was operated on the surface of the PSF–UF sheet membrane to fabricate the NF composite membranes. First, the PSF membrane was dipped into a blend aqueous solution of 2 wt % PIP and taurine (0–1 wt %) for 10 min. Then, the membrane was taken out, and excess solution was drained off with filter paper. The film was dried in air for 5 min and immersed in a 0.1 wt % TMC *n*-hexane solution for 30 s to obtain a PA layer through the IP reaction. Afterward, the resulting membrane was air-dried for 30 min to allow *n*-hexane to evaporate. Finally, the membrane was washed with deionized (DI) water and stored in DI water for further investigation.

Characterizations

The chemical structures of the membranes were characterized with a Vector-22 Fourier transform infrared (FTIR) spectrometer (Bruker Co., Germany). All of the samples were dried thoroughly *in vacuo* at 60°C for 24 h before characterization. The X-ray photoelectron spectroscopy (XPS) data were obtained on an AXIS-Ultra instrument Kratos Analytical (Shimadzu, Japan).

Field emission scanning electron microscopy (SEM; S-4800, Hitachi, Japan) was used to analyze the surface and cross-sectional morphologies of the composite NFMs. The samples frozen in liquid nitrogen were broken and sputtered with gold before SEM observation.

Water contact angle measurements were performed by the sessile drop method with a contact angle meter (Drop Shape Analysis 100, Kruss BmbH Co., Germany). A syringe was used to place a 3-μL water droplet on the membrane surface. Tangent lines to both sides of the droplet static image were generated and averaged by the Drop Shape Analysis software. At least three readings at different locations on one surface were measured to get a reliable value.

NF Performance Tests

The membrane performance was investigated by a cross-flow module at 25°C (unless otherwise specified, the following chapters performance tests were carried out at 25°C) and 0.7 MPa. The membranes were prefiltered with DI water at 0.7 MPa to reach a steady state before testing. The films were evaluated with 2 g/L $MgSO_4$ and NaCl aqueous solutions. The solution conductivity was tested at appropriate intervals with permeated liquid collected by a small beaker. The conductivity meter was a DDS-11A instrument (Shanghai Honggai Instrument Plant, China).

F and *R* were calculated by eqs. (1) and (2):

$$F = \frac{J}{AT} \tag{1}$$

$$R = \left(1 - \frac{C_p}{C_f}\right) \times 100\% \tag{2}$$

where *J* is the volume of permeated water (L), *A* is the effective area of the membrane (m^2, 7.07 cm^2), *T* is the time used by the permeation of a fixed volume water (h). *F* was calculated from eq. (1). C_p and C_f are the salt concentrations of the permeate and the feed solution, respectively. These were measured with a conductance meter (EL30, Mettler Toledo, Switzerland). *R* was calculated from eq. (2). Each sheet of the membrane was tested three times over an arbitrarily selected position, and the average was recorded.

Antifouling Performance Measurements

The protein adsorption experiments were carried out with BSA solutions. BSA was dissolved in 1 g/L BSA solution (pH 8). The film was cut into an appropriate size and put in a test cell. Before recording data, we preloaded the membrane with pure water as the testing liquid under 0.7 MPa. Sixty minutes later, prefiltration was enough for the membrane to reach a steady flux. Sequentially, water was replaced by BSA/PBS solution, and then, the flux was measured once every 10 min continuously

Table I. Chemical Compositions of the PSF, NFM 1, NFM 2, NFM 3, and NFM 4 Membrane Surfaces

Membrane	Taurine/ PIP (m/m)	Atomic concentration (mol %)				
		C1s	N1s	O1s	S2s	O/N
PSF		77.35	2.93	14.94	2.49	
NFM 1	0/2	73.89	10.11	14.17	0	1.40
NFM 2	0.2/1.8	70.8	11.36	16.73	0.6	1.47
NFM 3	0.5/1.5	71.14	9.24	18.12	1	1.96
NFM 4	1/1	70.34	6.36	19.74	1.91	3.10

for 240 min. The obtained flux profile was used to analyze the BSA fouling behavior of the TFC membranes. The membrane was washed with DI water for 30 min; afterward, the pure F of the cleaned membrane was measured again.

The normalized flux (F_x) values of the films were calculated by the following equation:

$$F_x = J/J_0 \quad (3)$$

where J_0 and J are the water fluxes of the initial and time t in the filtration process, respectively.

RESULTS AND DISCUSSION

Characterization of XPS

The PA thin film was deposited on the PSF support via IP. PSF was chosen as a candidate for the support material because of its excellent physical and chemical properties compared to those of other commercial polymers. The reaction between the aqueous and organic solutions during IP is shown in Figure 1. Four samples were tested with different ratios of taurine to PIP (Table I) aqueous solution. The membranes were named NFM 1, NFM 2, NFM 3, and NFM 4 depending on their respective contents of taurine. The concentrations of N and O elements were increased compared with those of the original PSF layer. In particular, the introduction of taurine showed an enhanced density of O atoms in the surface.

As shown in Figure 2(c), the characteristic peaks of N and O at 400 and 532.08 eV, respectively, all increased because of the introduction of taurine compared to those shown in Figure 2(a). In addition, the peaks at 285.08 and 162 eV corresponded to the C_{1s} and S_{2p} peaks shown in both Figure 2(a) and 2(c), respectively.

As shown in Figure 2, there were apparent differences between the high-resolution XPS spectra for the C1s of the PSF [Figure 2(b)] and NFM 2 [Figure 2(d)] membranes. Typically, PSF the

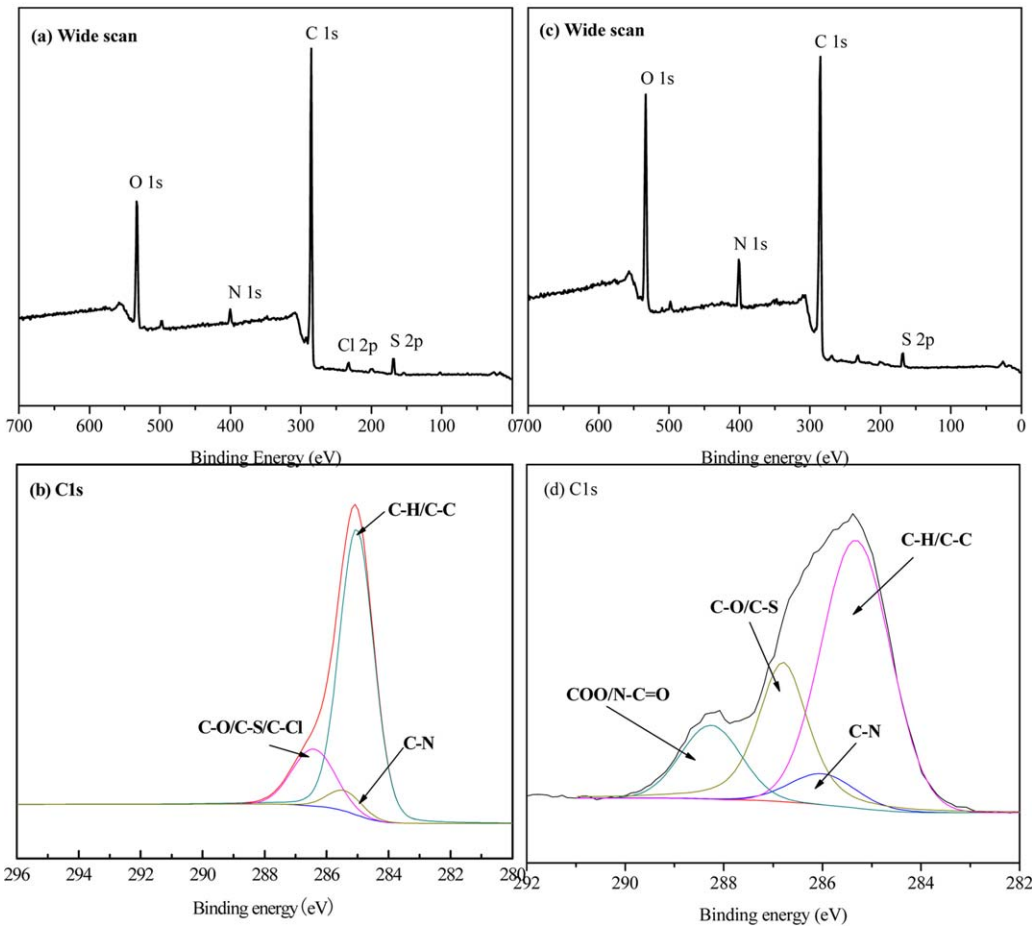

Figure 2. XPS spectra of the (a,b) PSF and (c,d) NFM 2 membrane surfaces. [Color figure can be viewed in the online issue, which is available at wileyonlinelibrary.com.]

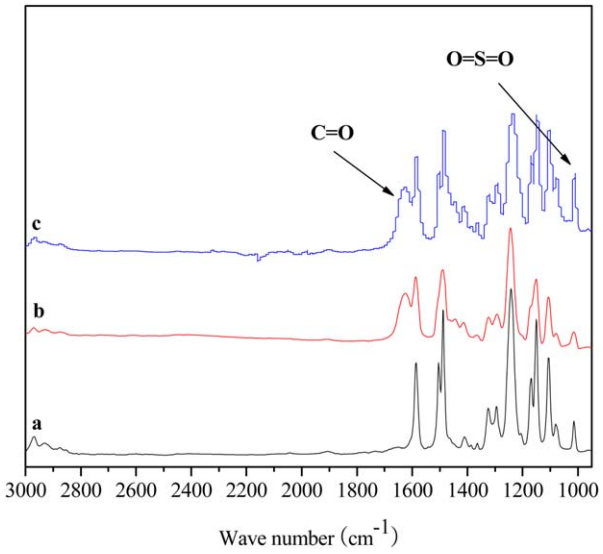

Figure 3. ATR–FTIR spectroscopy of the three TFC membranes and the PSF support membrane: (a) PSF, (b) NFM 1, and (c) NFM 2. [Color figure can be viewed in the online issue, which is available at wileyonlinelibrary.com.]

C1s spectrum showed three carbon moieties. The binding energy at 284.7 eV was assigned to the carbon skeleton (C—C/C—H), and those at 286.1 and 285.3 eV were attributed to C—O/C—S and C—N, respectively, in the PSF backbone. For C—N, as shown in Figure 2(b), there was evidence that there were poly(vinyl pyrrolidone) (PVP) residues in the membrane matrix. In the spectra shown in Figure 2(d), the peak at 286.1 eV (C—N) was dramatically larger than the one shown in Figure 2(b). Meanwhile, there were strong C—O/C—S and O—C=O/N—C=O peaks at 285.3 and 287.4 eV. It was further illustrated that a PA layer was formed on PSF.

Attenuated Total Reflectance (ATR)–FTIR Analysis

The PA thin film was confirmed to form on the PSF–UF sheet supporting layer by ATR–FTIR spectroscopy (Figure 3). In Figure 3(b,c), the new peak at 1628 cm^{-1} was characteristic of an amide of C=O;[19] this suggested a PA film formed robustly on the PSF basic membrane. In addition, the peak of 1029 cm^{-1} in Figure 3(c) was assigned to the stretching vibration band of O=S=O of $-SO_3H$; this confirmed that the PA surface was partially modified by taurine.

The pH of aqueous solutions and the molecular weight cutoff (Da) of membranes are shown in Table II. The aqueous solutions was alkaline, and with increasing taurine, the pH was reduced, and the molecular weight cutoff of membranes was enlarged; this reduced the rejection performance.

Surface and Cross-Sectional Morphologies of the NFMs

The cross-sectional and surface morphologies of the PSF membrane and the resulting composite membrane were characterized by SEM measurements, as shown in Figure 4. We observed that the composite membrane consisted of two distinctive layers, a dense layer coated on a porous support. Figure 4(a,a′) presents the surface morphologies of the PSF membrane and NFM 2, respectively. As observed, a grainy structure appeared on NFM 2 [Figure 4(b)], which may have arisen from stress during IP and swelling phenomena in the drying process. Figure 4(b,b′) represents the cross-sectional morphologies of the PSF membrane and NFM 2, respectively. We observed that there was a 100-nm PA layer on the skin of the UF membrane; this directly showed that a dense PA layer was successfully prepared on the substrate.

Water Contact Angle Measurement

Contact angle measurements were used to characterize the surface hydrophilicity of the membranes (Figure 5). The water contact angles of TFC membranes were all smaller than that of the PSF support. We observed that the water contact angles decreased rapidly with the taurine concentration, and meanwhile, the developing trend was gradually obvious with time; this indicated that the hydrophilicity increased with the concentration of taurine. The addition of taurine could have increased the hydrophilicity of the skin layer; this was crucial in ensuring the high fouling resistance.

NF Performance of the NFMs

Theoretically, a higher amine concentration could lead to fewer unreacted —COCl groups and thicken the membrane,[20] which would decrease *F*. However, in this study, it became complicated when taurine was incorporated as a hydrophilic additive to compete with PIP. As presented in Figure 6, *F* dramatically increased with the addition of taurine into the aqueous solution. When tested with a 2000-ppm NaCl solution, *F* of NFM 1 to NMF-4 increased from 26.8 to 35.5 L m^{-2} h^{-1}. The increase of flux was possibly due to increased hydrophilicity resulting from taurine. The sulfonate group could improve the surface hydrophilicity; this helped in the shackling of more free water. What is more, sulfonic acid also enhanced the negative charge on the surface, which helped to increase *F*.

R declined with increasing taurine content (Figure 7). For NFM 1 and NFM 2, the *R* values were stable at 92 and 33% for $MgSO_4$ and NaCl, respectively. However, the rejection of NFM 3 and NFM 4 were apparently affected by the taurine concentration. The hydrophilic additive increased not only the water permeability but also the permeation rate of inorganic ions. Taurine competed with PIP during the IP reaction; therefore, the ratio of taurine to PIP, rather than the PIP concentration alone, was used to analyze and explain the developing trends of *F* and *R*. This finding was supported by the incorporation of taurine into the membranes; despite the increasing membrane hydrophilicity, the incorporation of taurine could interfere with the IP of PIP. If the addition concentration was high enough (at low PIP/taurine concentration ratios); this resulted in a lower crosslink degree with a deteriorating desalination performance.

Table II. pH Values of the Aqueous Solutions for the Membrane Preparation and Molecular Weight Cutoff (Da) of the Membranes

Membrane	pH	Molecular weight cutoff (Da)
NFM 1	11.92	200-400
NFM 2	11.22	400-600
NFM 3	10.87	800
NFM 4	10.13	1000

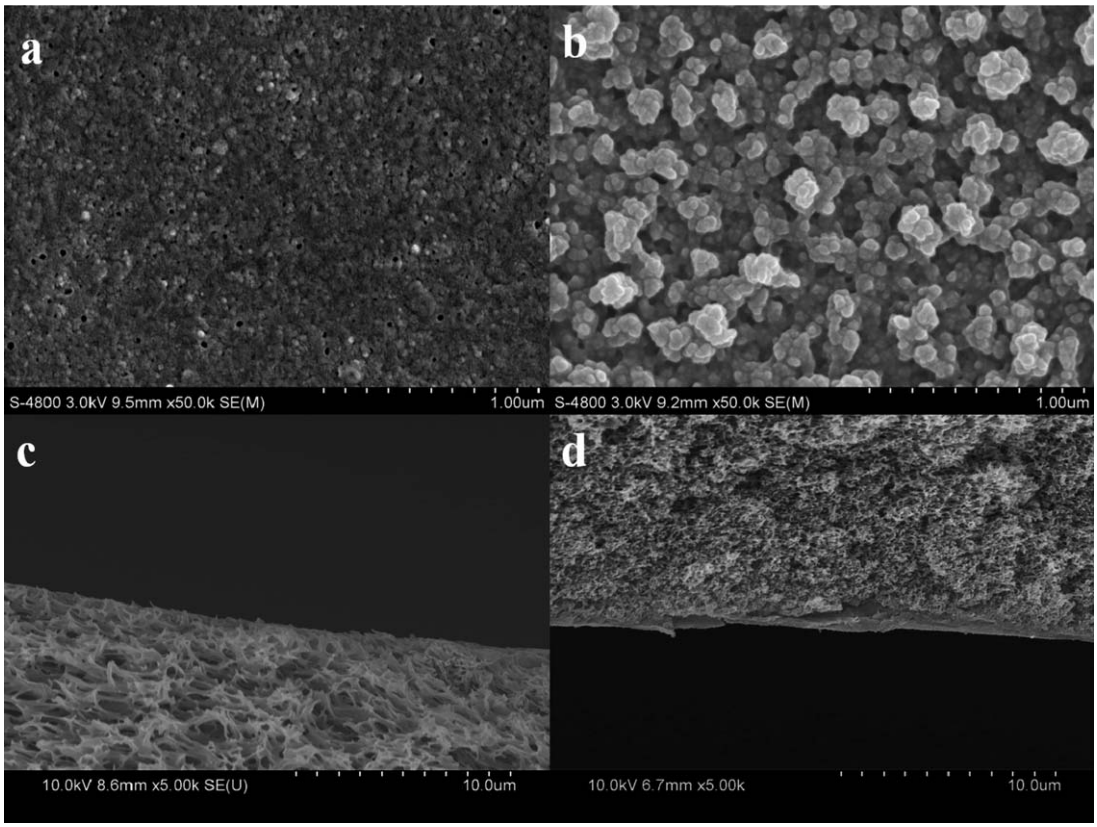

Figure 4. SEM images of the surface and cross-sectional morphologies: (a,c) PSF and (b,d) NFM 2.

Surface Charge

The surface charge properties of NFM 1 and NFM 2 were measured by a streaming method.[21] The results are presented in Figure 8. Both NFM 1 and NFM 2 showed typical amphoteric characteristics, with the positive charge contributed by residual amine groups and negative charges contributed by residual carboxylic groups and sulfonic acid groups. NFM 2 had a slightly more negative surface than NFM 1 because the negative charges of NFM 2 were contributed by the residual carboxylic group and sulfonic acid group, whereas the negative charges of NFM 1 were only contributed by residue carboxylic groups.

Antifouling Performance of the NFMs

The antifouling properties are very important for the practical application of NFMs. BSA was chosen as a model protein in water to evaluate the antifouling properties of the PA NFM.

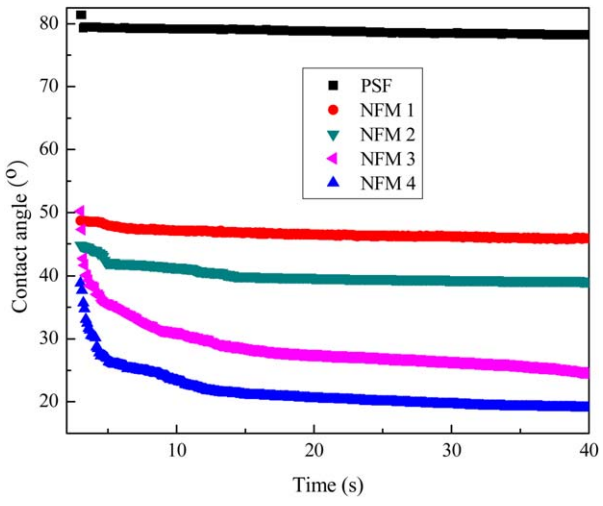

Figure 5. Water contact angles of the PSF and NFMs. [Color figure can be viewed in the online issue, which is available at wileyonlinelibrary.com.]

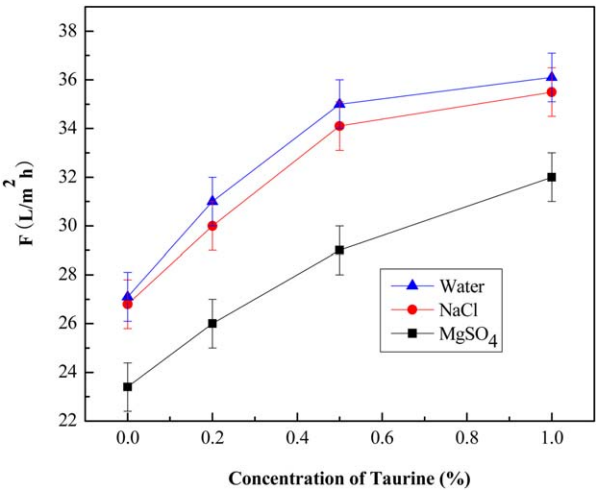

Figure 6. *F* performance of the NFMs tested with DI water and different inorganic salt aqueous solutions (2000 ppm) at 25°C and 0.7 MPa. [Color figure can be viewed in the online issue, which is available at wileyonlinelibrary.com.]

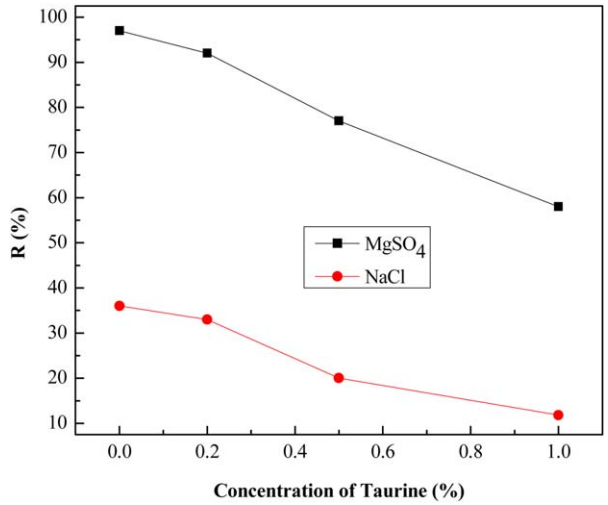

Figure 7. *R* performance of the NFMs tested with different inorganic salt aqueous solutions (2000 ppm) at 25°C and 0.7 MPa. [Color figure can be viewed in the online issue, which is available at wileyonlinelibrary.com.]

Figure 9 shows the evolution of the flux within the filtration time of 240 min. The permeation flux dropped very quickly. This happened to both the NFM 1 and NFM 2 membranes. However, much lesser fouling occurred with the NFM 2 membrane. After 240 min, NFM 2 lost about 34% of the initial flux, whereas the NFM 1 membrane lost almost 42% of its initial flux. After the cleaning experiments of BSA filtration with DI water rinsing, NFM 2 recovered it is lost *F* to over 99%. On the contrary, the flux of NFM 1 recovered just to 88% of its initial value. This was attributed to the more hydrophilic surface built by taurine and the electronic repulsion between the negatively charged membrane surface and BSA under the testing pH. The introduction of the sulfonic group increased the hydrophilicity and negative charges on the membrane surface. The increased hydrophilicity and charges increased the binding force to free water and repellence to charged protein and made the membranes easy to clean.[21]

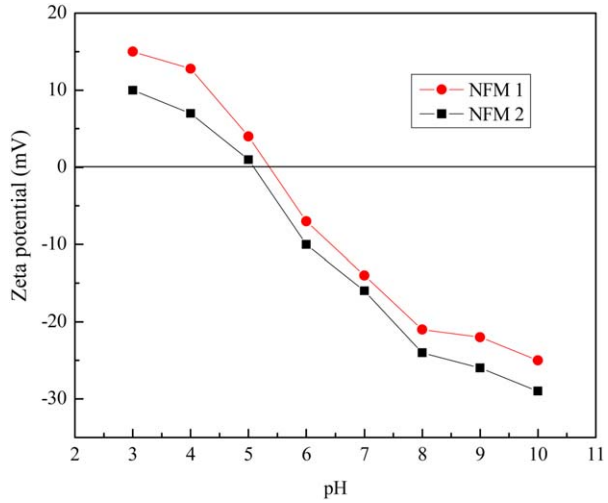

Figure 8. ζ potentials for NFM 1 and NFM 2. [Color figure can be viewed in the online issue, which is available at wileyonlinelibrary.com.]

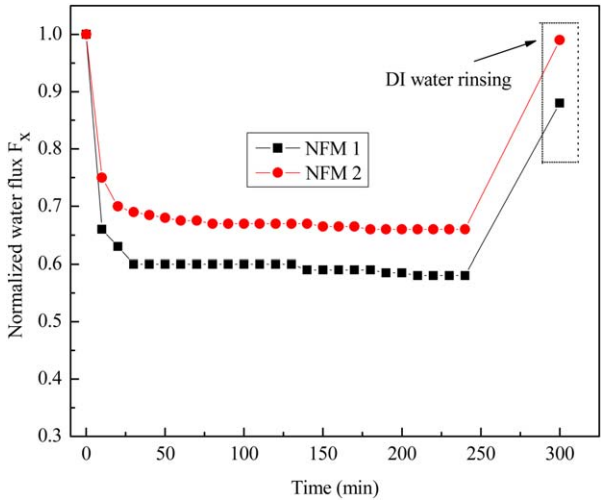

Figure 9. Antifouling performance of the NFMs tested with DI water and a BSA/PBS aqueous solution (pH = 8) at 25°C and 0.7 MPa. [Color figure can be viewed in the online issue, which is available at wileyonlinelibrary.com.]

CONCLUSIONS

Antipollution TFC NFMs were prepared with taurine as an additive. The introduction of taurine increased the surface hydrophilicity and surface negative charge of the composite membranes. The water contact angles decreased rapidly with the taurine concentration. Meanwhile, the developing trend was gradually obvious with the time. However, an overdose of monofunctional taurine captured more COCl groups; this decreased the crosslinking degree and affected *R* finally. Membranes showing typical amphoteric characteristic of charge for TFC membranes, membrane surface negative charges, and enhancement of the hydrophilicity improved the antifouling performance of the NFMs. Taurine aqueous solution (0.2 wt %, NFM 2) showed 92% $MgSO_4$ rejection at 31 L m^{-2} h^{-1} and a better antifouling performance (NFM 2 recovered its lost *F* to over 99% after DI water rinsing).

ACKNOWLEDGMENTS

This research was supported by China High-Tech R&D Program (863 Program, contract grant number 2012AA03A602).

REFERENCES

1. McCutcheon, J. R.; McGinnis, R. L.; Elimelech, M. *Desalination* **2005**, *174*, 1.
2. McCutcheon, J. R.; McGinnis, R. L.; Elimelech, M. *J. Membr. Sci.* **2006**, *278*, 114.
3. Cath, T. Y.; Childress, A. E.; Elimelech, M. *J. Membr. Sci.* **2006**, *281*, 70.
4. Zhong, P. S.; Widjojo, N.; Chung, T.; Weber, M.; Maletzko, C. *J. Membr. Sci.* **2012**, *417*, 52.
5. Shao, L.; Cheng, X. Q.; Liu, Y.; Quan, S.; Ma, J.; Zhao, S. Z.; Wang, K. Y. *J. Membr. Sci.* **2013**, *430*, 96.
6. Fang, W.; Shi, L.; Wang, R. *J. Membr. Sci.* **2013**, *430*, 129.

7. Vrouwenvelder, J. S.; van der Kooij, D. *Desalination* **2001**, *139*, 65.
8. Park, N.; Kwon, B.; Kim, I. S.; Cho, J. *J. Membr. Sci.* **2005**, *258*, 43.
9. Ivnitsky, H.; Katz, I.; Minz, D.; Shimoni, E.; Chen, Y.; Tarchitzky, J.; Semiat, R.; Dosoretz, C. G. *Desalination* **2005**, *185*, 255.
10. Lee, S.; Boo, C.; Elimelech, M.; Hong, S. *J. Membr. Sci.* **2010**, *365*, 34.
11. McGinnis, R. L.; Elimelech, M. *Desalination* **2007**, *207*, 370.
12. Emadzadeh, D.; Lau, W. J.; Ismail, A. F. *J. Membr. Sci.* **2014**, *449*, 74.
13. Zhao, J.; Su, Y.; Jiang, Z. *J. Membr. Sci.* **2014**, *465*, 41.
14. Li, X.; Cao, Y. *J. Membr. Sci.* **2014**, *466*, 82.
15. Zhao, L.; Philip, C.-Y.; Chang, W. S.; Ho, W. *Desalination* **2013**, *308*, 225.
16. Kim, I.-C.; Jeong, B.-R.; Kim, S.-J.; Lee, K.-H. *Desalination* **2013**, *308*, 111.
17. Kuehne, M. A.; Song, R. Q.; Li, N. N.; Petersen, R. *J. Environ. Prog.* **2001**, *20*, 23.
18. Zheng, J.; He, Q.; Gao, N.; Yuan, T.; Zhang, S. *J. Membr. Sci.* **2014**, *261*, 38.
19. Klaysom, C.; Hermans, S.; Gahlaut, A.; Craenenbroeck, S. V.; Vankelecom, I. F. J. *J. Membr. Sci.* **2013**, *445*, 25.
20. Klaysom, C.; Hermans, S.; Gahlaut, A.; VanCraenenbroeck, S.; Vankelecom, I. F. J. *J. Membr. Sci.* **2013**, *445*, 25.
21. Yao, F.; Fu, G.-D.; Zhao, J.; Kang, E.-T.; Neoh, K. G. *J. Membr. Sci.* **2008**, *319*, 149.